

# Future perspectives for $\mu^+ \rightarrow e^+\gamma$ searches

Contact Persons: Waratu Ootani<sup>1</sup> and Francesco Renga<sup>2</sup>

<sup>1</sup> ICEPP, The University of Tokyo,  
7-3-1 Hongo, Bunkyo-ku, Tokyo 113-0033, Japan  
wataru@icepp.s.u-tokyo.ac.jp

<sup>2</sup> INFN Sezione di Roma,  
Piazzale A. Moro 2, 00185 Roma, Italy  
francesco.renga@roma1.infn.it

## Abstract

Searches for charged lepton flavor violation in the muon sector stand out among the most sensitive and clean probes for physics beyond the Standard Model. Currently,  $\mu^+ \rightarrow e^+\gamma$  experiments provide the best constraints in this field and, in the coming years, new experiments investigating the processes of  $\mu^+ \rightarrow e^+e^+e^-$  and  $\mu \rightarrow e$  conversion in the nuclear field are anticipated to surpass them. However, it is essential to maintain comparable sensitivities across all these processes to fully leverage their potential and differentiate between various new physics models if a discovery occurs. In this document, we present ongoing efforts to develop a future experimental program aimed at improving the sensitivity of  $\mu^+ \rightarrow e^+\gamma$  searches by one order of magnitude within the next decade.

## EDITORS

Paolo Walter Cattaneo,<sup>1</sup> Giovanni Dal Maso,<sup>2</sup> Matteo De Gerone,<sup>3</sup> Wataru Ootani,<sup>4</sup>  
Atsushi Oya,<sup>4</sup> Angela Papa,<sup>5</sup> Francesco Renga<sup>6</sup> and Andre Schöning<sup>7</sup>

<sup>1</sup> INFN Sezione di Pavia, Via Bassi 6, 27100 Pavia, Italy

<sup>2</sup> CERN, Geneva, Switzerland

<sup>3</sup> INFN Sezione di Genova, Via Dodecaneso 33, 16146 Genova, Italy

<sup>4</sup> ICEPP, The University of Tokyo, 7-3-1 Hongo, Bunkyo-ku, Tokyo 113-0033, Japan

<sup>5</sup> INFN Sezione di Pisa and Dipartimento di Fisica dell'Università,  
Largo B. Pontecorvo 3, 56127 Pisa, Italy

<sup>6</sup> INFN Sezione di Roma, Piazzale A. Moro 2, 00185 Roma, Italy

<sup>7</sup> Physikalisches Institut, Universität Heidelberg, Im Neuenheimer Feld 226, 69120 Heidelberg,  
Germany

on behalf of the Study Group for Future  $\mu^+ \rightarrow e^+\gamma$  Experiments

## 1 Introduction

In the standard model (SM) of particle physics, charged lepton flavour-violating (cLFV) processes are basically forbidden with only extremely small branching ratios ( $\sim 1 \times 10^{-54}$  [1]) when accounting for non-zero neutrino mass differences and mixing angles. However, being the conservation of the lepton flavor an accidental symmetry in the SM, several New Physics (NP) extensions predict cLFV decays at measurable rates, and the channel  $\mu^+ \rightarrow e^+\gamma$  is particularly sensitive. Thus, such decays serve as an excellent probe for NP, due to their high sensitivity and the absence of SM contributions, making any potential positive signal unequivocal evidence for physics beyond the SM. Reviews of the theoretical expectations and experimental status are provided in [1, 2].

The MEG and MEG II experiments set the best limit on the branching ratio of the  $\mu^+ \rightarrow e^+\gamma$  decay,  $\mathcal{B}(\mu^+ \rightarrow e^+\gamma) < 3.1 \times 10^{-13}$  at 90% confidence level [3], currently dominating the cLFV constraints in the muon sector. MEG II is expected to continue taking data in 2025 and 2026, reaching a sensitivity of  $6 \times 10^{-14}$ . In the meanwhile the Mu3e [4], Mu2e [5] and COMET [6] collaborations are finalizing the construction of their detectors to search for the  $\mu^+ \rightarrow e^+e^+e^-$  decay and the  $\mu^-N \rightarrow e^-N$  conversion in the Coulomb field of nuclei, with sensitivities to NP potentially overcoming the MEG II one. However, given the possibly different NP contributions to these processes ( $\mu^+ \rightarrow e^+\gamma$  requires a dipole-like vertex, while the others can also go through an effective four-fermion contact interaction), these searches are complementary. If an observation is made in one of these experiments, only the results of the others will allow to discriminate between different NP models. This is only possible if their sensitivities (in terms of NP mass scale) are at comparable levels. That requires the development of a program to improve by at least one order of magnitude the sensitivity of the  $\mu^+ \rightarrow e^+\gamma$  search.

In this document, we report the current status of ongoing activities toward a future  $\mu^+ \rightarrow e^+\gamma$  experiment, exploiting the high intensity muon rates that will be available after the upgrades of the existing muon beam facilities.

## 2 Current experimental status

The MEG II experiment, currently being conducted at the Paul Scherrer Institute (PSI), is the most sensitive  $\mu^+ \rightarrow e^+\gamma$  search to date. The extremely high sensitivity of MEG II relies on the high intensity continuous muon beams available at PSI and the innovative detectors identifying photons and positrons with exceptional precisions in the energy, timing, and spatial reconstructions. The MEG II experiment was upgraded from MEG, retaining the experimental concept but with significantly improved detector performance (Fig. 1) [7, 8].

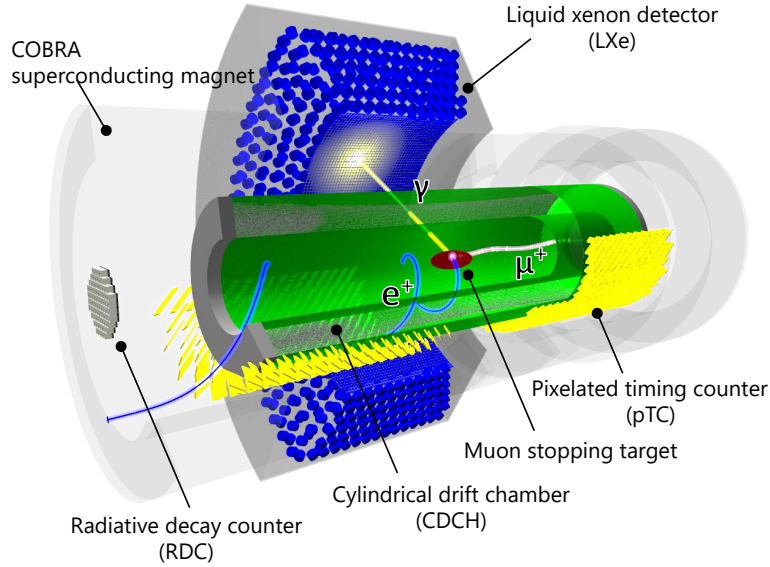


Figure 1: The MEG II experiment [7, 8].

The decays of muons stopped in a thin target at a rate of  $(3 - 5) \times 10^7 \mu^+ / s$  are measured by the positron and photon detectors surrounding the target with a solid angle coverage of 10%. The positron detector is a magnetic spectrometer with a gradient magnetic field designed to quickly sweep away low-momentum Michel positrons from the tracking volume. The positrons are precisely tracked by a low-mass single-volume cylindrical drift chamber with a stereo wire configuration to form high-granularity drift cells. The positron timing is measured by a segmented timing detector composed of 512 fast scintillator tiles read out by Silicon PhotoMultipliers (SiPMs). The signal positron passes through multiple scintillator tiles in the detector. An excellent timing resolution is achieved by averaging the times measured by the multiple tiles. The energy, timing, and impinging position of the photon are measured by liquid xenon (LXe) calorimeter with a single-volume 900L LXe surrounded by VUV-sensitive photosensors; 4092 MPPCs ( $12 \times 12 \text{ mm}^2$ ) on the front face for fine photon imaging and 668 PMTs (2-inch) on the other faces. A new detector, Radiative Decay Counter (RDC), was introduced in MEG II to further suppress the photon backgrounds from the radiative muon decays (RMD) by identifying low momentum Michel positrons associated to RMD photons around the signal photon energy. The RDC, composed of plastic scintillators for timing and LYSO crystals for energy measurements, is placed on the beam axis only at the downstream end.

### 3 Beam availability

Experiments dedicated to search for rare decays, such as MEG and  $\text{Mu}3e$ , require the collection of high statistics to achieve their sensitivity goals. The High Intensity Proton Accelerator (HIPA) facility at the Paul Scherrer Institut (PSI) has been leading research at the high-intensity frontier for decades by delivering surface muon beam rates up to a few  $10^8 \mu^+ / s$ . In the future, new experimental efforts, like those proposed in this document, will require ever-higher beam intensities, and the High Intensity Muon Beams (HIMB) project [9] aims at improving the currently available rates by two orders of magnitude, up to  $10^{10} \mu^+ / s$ . The next generation of proton drivers to deliver beam power greater than 1.4 MW requires significant research and development, so the HIMB project aims to improve the delivered surface muon rates by increasing the muon yield with a new target geometry [10, 11] and improving both the capture and transmission efficiencies with a beamline based on large aperture solenoids.

The new target station TgH will substitute the current TgM, increasing the target length from

5 mm to 20 mm in the direction of the proton beam. A  $10^\circ$  slanting angle will be introduced with respect to the proton beam direction to increase the surface to volume ratio of the target thus boosting the surface muon yield. Two beamlines will capture muons at  $90^\circ$  with respect to the proton beam. The MUH2 beamline will replace the  $\pi M1$  area and will deliver the highest intensity beams for particle physics experiments, and is therefore the most appealing for future  $\mu^+ \rightarrow e^+\gamma$  searches. The MUH3 beamline will replace the  $\pi M3$  and serve  $\mu SR$  instruments. Figure 2 shows the layout of the HIPA facility including the HIMB beamlines. HIMB will be installed at the HIPA shutdown during 2027-2028.

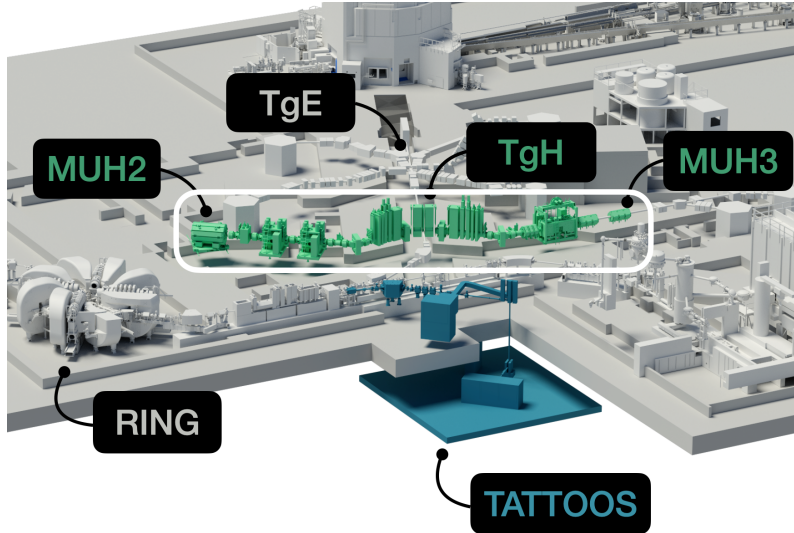


Figure 2: Overview of the HIPA accelerator complex including the HIMB beamlines and the new isotope production target station TATTOOS. The new target station TgH will replace the current TgM and the beamlines will replace  $\pi M1$  and  $\pi M3$ . Adapted from [9].

A technical design report is currently under preparation and will be implemented during a long shutdown of HIPA in 2027-2028. The current designs of MUH2 will allow to deliver up to  $\sim 1.10 \times 10^{10} \mu^+ / s$  with a  $1\sigma$  beam spot size on target of  $35 \text{ mm} \times 35 \text{ mm}$  and a positron contamination lower than 5%. In addition, the beamline is designed to deliver particles with momenta up to  $80 \text{ MeV}/c$  and with the possibility to switch to electron, positron and charged pion beams for further experimental application [12, 13].

## 4 Experimental approach

### 4.1 Experimental concept

As in MEG and MEG II, the experimental concept is based on reconstructing photons and positrons from muons decaying at rest in a thin stopping target. The two-body kinematics will be exploited to discriminate backgrounds from accidental coincidences (the dominant source) and radiative muon decays. It requires excellent resolutions on photon and positron energies, their directions and their relative emission time.

The best reconstruction of positron energy and direction is offered by magnetic spectrometers. Given the relatively low momentum of signal positrons ( $52.8 \text{ MeV}/c$ ), stochastic effects in their interaction with the detector materials play a critical role in determining the achievable resolutions. At the state of the art, gaseous detectors with helium-based mixtures guarantee the best compromise of single-hit resolution and material budget. However, drift chambers have limited rate capabilities due to poor granularity and ageing effects, while conventional time projection chambers (TPCs) cannot provide the necessary single-hit resolutions when operated with helium [14]. Although alternative geometries could be considered (as, for instance, TPCs with a radial drift field), we are taking the use of silicon pixel detectors as a baseline solution for positron tracking. Indeed,

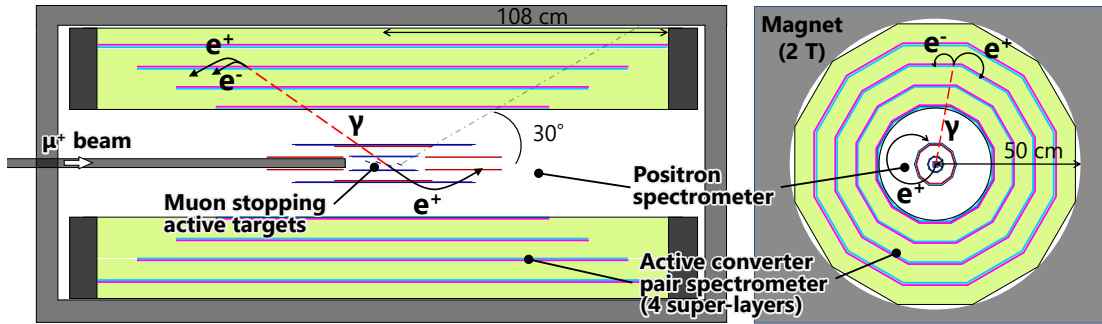


Figure 3: A sketch of a detector for  $\mu^+ \rightarrow e^+\gamma$  decays with a silicon pixel tracker for positrons, and active conversion layers with  $e^+e^-$  trackers for photons.

R&D studies are being performed in the context of the Mu3e Phase II upgrade project [12] aiming to further reduce the material of ultra-thin tracking detectors which are based on High Voltage Monolithic Active Pixel Sensors (HVMAPS) [15] and have 0.1% radiation length or less.

On the photon side, the performance of the LXe calorimeter of MEG and MEG II largely surpassed all previous experiments. However, there is no clear path to further improve the photon energy resolution in this kind of detector. Innovative crystals like LYSO could provide better performance, and R&D activities are ongoing on small prototypes [16]. In this case, a limiting factor could be the technological capability of growing large crystals, and their cost. Hence, although this calorimetric approach can be a very interesting option for an intermediate phase in a staged approach (see Sec. 6), we are considering a different approach as a baseline: a layer of dense material would be used to convert photons into  $e^+e^-$  pairs, subsequently tracked in a magnetic spectrometer. In principle, an excellent momentum resolution can be achieved on the  $e^+e^-$  pair. However, if a passive conversion layer is used, the energy loss fluctuations in the converter itself limit the energy resolution [17]. It calls for a very thin conversion layer, resulting in poor conversion efficiency. As an alternative, we are proposing to adopt thin LYSO crystals readout by SiPM as active converters, where the energy loss can be measured and used to correct the energy reconstructed in a gaseous  $e^+e^-$  spectrometer. The residual efficiency loss compared to calorimeters can be compensated by superimposing several conversion and tracking layers, and increasing the beam rate.

A sketch of a detector based on these techniques is presented in Fig. 3. The technological aspects of the proposed approaches and their expected performance will be discussed in the next sections.

## 4.2 Photon reconstruction

### 4.2.1 Calorimeter experiments

Two very promising materials as BrillLanCe (Cerium doped Lanthanum Bromide,  $\text{LaBr}_3(\text{Ce})$ ) and LYSO (Lutetium Yttrium OxyorthoSilicate,  $\text{Lu}_{2(1-x)}\text{Y}_{2x}\text{SiO}_5(\text{Ce})$ ) coupled to Silicon Photomultipliers (MPPC/SiPM) could represent an appealing option for the future calorimeter. The response of both  $\text{LaBr}_3(\text{Ce})$  and LYSO detectors read out by SiPMs have been studied via detailed Monte Carlo (MC) simulations based on GEANT4. The impinging gammas are in the range of 50-100 MeV. The MC simulations includes the full read out chain up to the waveform digitizer and is followed by the reconstruction algorithms.

The results that have been obtained are very promising. For a cylindrical crystal (radius  $R = 4.45$  cm, length  $L = 20.3$  cm)  $\text{LaBr}_3(\text{Ce})$  crystal an energy resolution of  $\sigma_E/E [\%] = 2.3(1)$  and a timing resolution of  $\sigma_t = (35 \pm 1)$  ps have been predicted. The energy resolution can be further improved by using larger crystals (either  $R = 6.35$  cm or  $R = 7.6$  cm,  $L = 20.3$  cm) approaching respectively  $\sigma_E/E = (1.20 \pm 0.03) \%$  or  $\sigma_E/E = (0.91 \pm 0.01) \%$ . Detector based on LYSO crystal of similar size performs even better, thanks to the shorter LYSO Moliere radius compared to  $\text{LaBr}_3(\text{Ce})$ . For a detector based on a ( $R = 3.5$  cm,  $L = 16$  cm) LYSO crystal an energy resolution of

$\sigma_E/E$  [%] = 1.7(1)% can be obtained, and that can be further improved using bigger crystals ( $R = 6.5$  cm,  $L = 25$  cm,  $\sigma_E/E$  [%] = 0.74(1)%). Energy resolution approaching  $\sigma_E/E$  [%] = 0.3(1)% can be addressed for both crystals with ultimate sizes ( $R = 20$  cm – 23 cm,  $L = 17$  cm – 32 cm), complemented by timing and position resolutions in the range of  $O(30)$  ps and  $O(\text{a few mm})$  respectively. Such results put these future high energy calorimeters at the detector forefront at intensity frontiers.

Based on the availability of crystals on the market, we focused on building a first calorimeter prototype using LYSO crystals. Figure 4 shows a sketch of the detector, which uses a LYSO crystal having a 4.25 cm diameter and a 10 cm length, following a double readout scheme with SiPMs coupled to both the front and back faces of the cylindrical detector.

Figure 5 shows the ultimate resolutions that could be achieved with either a  $\text{LaBr}_3(\text{Ce})$  or LYSO option, using the crystal sizes as reported in the caption.

#### 4.2.2 Conversion experiments

A conversion pair spectrometer is currently considered the baseline option for the photon measurement since it is more advantageous for future  $\mu^+ \rightarrow e^+\gamma$  experiments with higher beam rates. The photon is converted into an  $e^+e^-$  pair in a thin conversion layer, and the conversion pair is precisely tracked by a magnetic spectrometer. The energy resolution is, therefore, expected to be much higher than the calorimetric option. The photon hit position can also be more precisely measured by the reconstructed tracks. Another advantage would be the capability of measuring the photon incident angle with the reconstructed tracks, which can further suppress accidental backgrounds. On the other hand, the limiting factors for the conversion spectrometer are the low detection efficiency and the energy loss by the conversion pair in the converter. The low detection efficiency can be compensated by multiple conversion layers and higher beam rates while suppressing accidental backgrounds with the higher resolutions. For the issue of the energy loss in the converter, an active converter is proposed where the energy loss is measured by the converter itself, which is used to correct the energy measured by the conversion pair tracker (Fig. 6). Since the energy loss in the converter is a small portion of the initial photon energy, very high energy resolution is not required for the active converter. The active converter can also work as a photon timing detector. The photon timing can be measured by the hit time of the conversion pair returning to the active converter.

Heavy scintillator crystals can be good candidates for the detector medium of the active converter with higher detection efficiency. LYSO is considered the best candidate among standard crystals thanks to its high light yield and fast response. A simulation study shows a detection efficiency of a few % with an optimal thickness of 3 mm. The cylindrical conversion layer shown in Fig. 3 is segmented into small strips to mitigate the pileup of background photons and the effect of

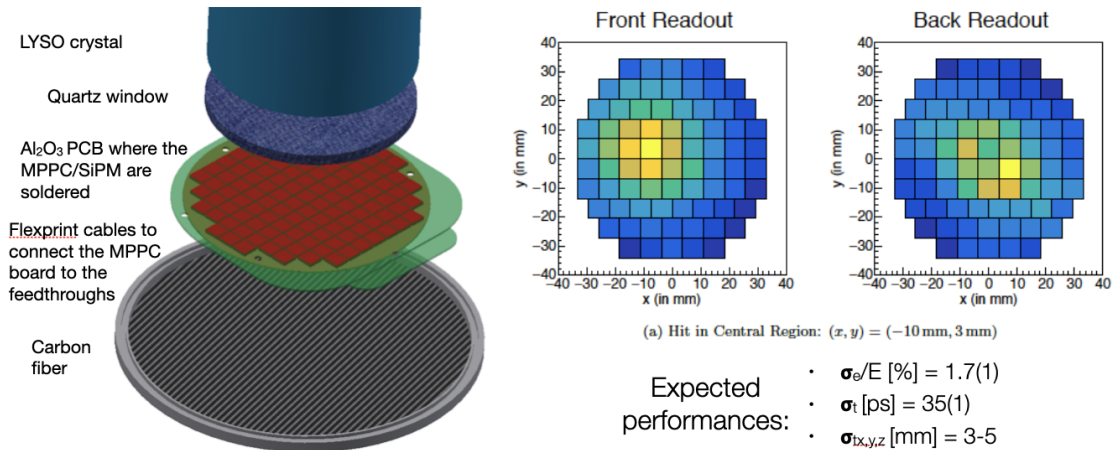


Figure 4: A sketch of a LYSO crystal prototype having a 4.25 cm diameter and 10 cm length with the details of the photosensor coupling.

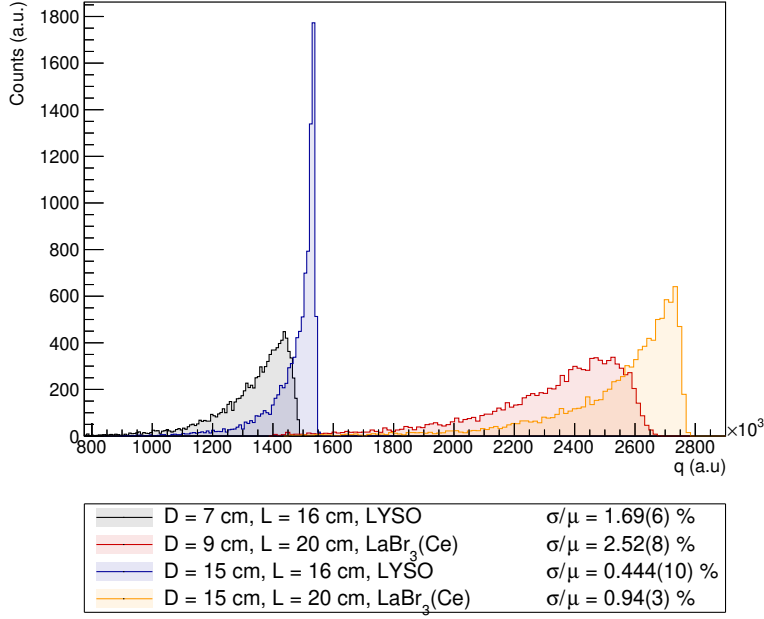


Figure 5: *Expected energy resolutions for different LaBr<sub>3</sub>(Ce) or LYSO options.*

the returning conversion pair on the energy loss measurement. The optimal segmentation is found in simulation studies to be  $5 \times 50 \text{ cm}^2$ . The performance of the LYSO strips was measured in the KEK AR Test Beam Line in December 2024. Figure 7 shows the single MIP time resolution of a LYSO strip of  $5 \times 50 \times 3 \text{ mm}^3$  read out at both ends by SiPMs (Hamamatsu MPPC S14160-6050HS  $6 \times 6 \text{ mm}^2$ ) measured with 3 GeV electrons. Excellent time resolution of  $\sim 28 \text{ ps}$  is achieved over the entire strip except for the edge. Since the photon timing is measured by both the electron and positron from the conversion, the time resolution is expected to be  $\sim 20 \text{ ps}$ , significantly improved in comparison with the time resolution of the MEG II LXe photon calorimeter of  $\sim 65 \text{ ps}$ . The light yield of the LYSO strip was also measured to be so high that the contribution of the Poisson fluctuation in the number of photoelectrons is negligibly small not to spoil the precise energy reconstruction of the conversion pair by the tracker.

Tracks from photon conversion will be emitted in a wide energy spectrum, and with a possibly large energy asymmetry between the  $e^+$  and the  $e^-$ . Consequently, in order to guarantee high resolution and reconstruction efficiency, extremely light pair trackers in a magnetic field are needed, covering a relatively large range of bending radii. Since the photon converter layers located outside the positron spectrometer are not in a harsh environment, gaseous detectors can be used, providing the best possible tracking performance (thanks to the low material budget) at a relatively low cost. However, the limited granularity of wire chambers would make them inefficient in the low end of the energy spectrum. For their part, conventional time projection chambers (TPC), with electrons drifting up to 1 m along the magnetic field, require mixtures like Ar-CO<sub>2</sub> for a sufficiently low diffusion, which would be too heavy for this application. We propose to adopt an unconventional design where electrons drift radially, for no more than 10 cm, and are multiplied in cylindrical micro-pattern gaseous detectors (MPGD). The short drift distance helps to maintain low diffusion levels, even in light, helium-based gas mixtures. Additionally, the anticipated low occupancy enables the use of stereo strips instead of pads for the readout, which helps to reduce the number of electronic channels required. The recent advancement in cylindrical Gas Electron Multipliers (GEMs) has paved the way for this application. However, R&D studies are needed for constructing cylindrical MPGDs with diameters exceeding 1 m. Moreover, intriguing challenges arise in hit reconstruction and pattern recognition when using strip readout on drift distances extending over several centimeters. Simulations show that, with a single hit resolution around  $500 \mu\text{m}$ , which is a reasonable target for this kind of detectors, a resolution around 0.3 % can be reached on the  $e^+e^-$  energy sum after the energy loss in the converter. Hardware R&D activities have been already

initiated to study the performance of TPCs with O(10 cm) drift and a strip readout.

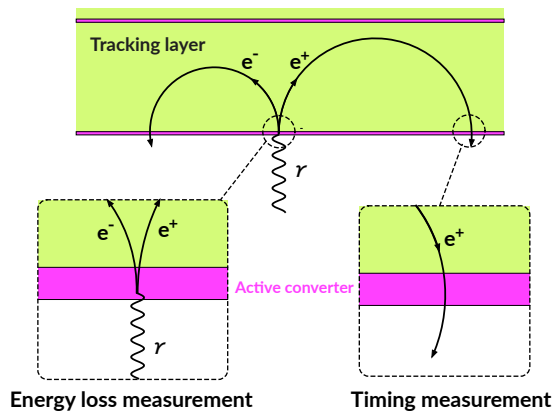


Figure 6: Concept of the active converter.

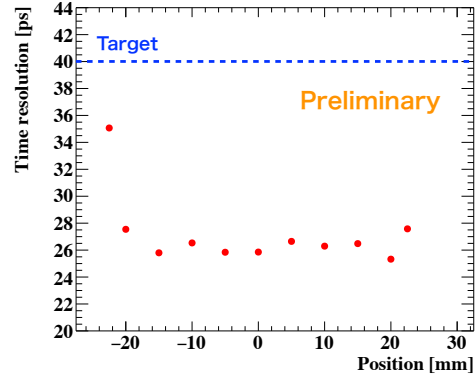


Figure 7: Single MIP time resolutions for LYSO strip of  $5 \text{ mm} \times 50 \text{ mm} \times 3 \text{ mm}$ .

## 4.3 Positron reconstruction

### 4.3.1 Positron tracking

Due to their high rate capability and granularity, silicon pixel sensors are the best choice for tracking positrons from muon decays at muon stopping rates up to  $10^{10} \text{ s}^{-1}$ , as expected at HIMB. For a positron momentum of  $p = 52.83 \text{ MeV}/c$ , as given by the  $\mu^+ \rightarrow e^+ \gamma$  2-body decay, the momentum resolution is dominated by multiple Coulomb scattering (MS). In this regime, the best momentum resolution is achieved with a tracking detector design similar to that used in the Mu3e experiment, where recurving tracks are measured after a  $180^\circ$  free bend. Using ultra-thin HVMAPS, which are as thin as  $\sim 50 \mu\text{m}$ , a momentum resolution of O(100 keV/c) can be achieved in a strong magnetic field of  $B = 2 \text{ T}$ . For track finding, four or better five tracking layers will be required to keep the rate of wrong hit combinations under control. Similar to the Mu3e pixel tracker, gaseous helium will be used for detector cooling, as it has the smallest radiation length of all known cooling technologies.

The second important handle for suppressing the accidental background is the accurate measurement of the electron-photon back-to-back topology. For this, the vertexing capability of the thin HVMAPS tracking layers, which is determined by the pixel size and the material thickness of the innermost tracking layer, and the thickness of the muon stopping target are of key importance. For a wide muon stopping target, which is required to fully exploit the high muon rates of HIMB, the vertex resolution will be dominated by the extrapolation uncertainty coming from MS in the innermost tracking layer. This can be remedied by an active muon stopping target, where the position of the muon decay is directly measured. Such an active target must be very thin and needs an extremely high rate capability to stand the high HIMB rates. A natural technology choice are also HVMAPS, which are highly radiation tolerant [18]. However, significant R&D will be required to develop such a detector.

If we consider scenarios where the experiment is run with about  $10^8 \mu^+/\text{s}$ , a conventional gaseous detector similar to the MEG-II drift chamber, and hence not requiring an extensive R&D effort, could be employed for positron tracking. Research is currently underway on low-aging gas mixtures and innovative pattern recognition tools that use machine learning for track reconstruction. The goal is to demonstrate that such a detector can be safely and effectively operated at a beam rate more than twice that of MEG II.

Alternative options for tracking positrons at rates of up to  $10^9 \mu^+/\text{s}$  are also being considered. In this context, the advantages of a radial TPC over wire chambers could be effective once again. However, there are additional challenges posed by the extremely high occupancy levels. First, it would be essential to read the MPGDs using pads. This requirement, combined with a radial configuration, necessitates the development of highly compact electronics that can be placed on

the external surface of the chamber without compromising the performance of the external detectors. Second, the substantial space charge that accumulates within the drift region would require advanced calibration and analysis tools, which have not yet been studied for the unconventional radial configuration.

### 4.3.2 Positron timing

The timing of the positron must be measured to be matched with the photon timing to suppress the accidental background resulting from two different muons decaying close in time, one in a high energy positron and one in a high energy photon. The timing of the positron cannot be measured close to the production point on the target because the tracking technologies under consideration do not provide an adequate resolution. The requirement on positron timing resolution are dictated by the photon timing resolution: it must be comparable or somehow better. From Sect. 4.2.2, where we assume a photon timing resolution less than 30 ps, the design goal of the positron timing detector is  $\sim 20$  ps. We also have to make sure that the correction for the positron time of flight to the decay target adds a small contribution to the resolution.

The resolution of the pTC in MEG II  $\sim 30$  ps [8] is already close to the requirements. That is obtained relying on plastic scintillator pixels readout on opposite sides by array of SiPMs. They are arranged in such a way that several ( $\sim 9$ ) are traversed by signal positrons. A resolution improvement can be achieved by reducing the size of the pixels, increasing their thickness, the number of SiPM, the SiPM size. Alternatively, the design of Mu3e can be considered, where one or two cylindrical layers of small scintillating cubes ( $1 \times 1 \times 1 \text{ cm}^3$ ) are readout by a single SiPM; again the signal positron is expected to cross multiple pixels. A focused R&D program with tests and simulations will determine the optimal balance between timing performance, cost, mechanical complexity and number of readout channels.

Alternative solutions for positron timing are also under study, thanks to the recent developments of fast timing detectors. The HVMAPS themselves could measure the positron time with a very good resolution. One of the HVMAPS tracking layers could also serve as a dedicated timing layer, providing a time resolution  $\lesssim 50$  ps per particle crossing, which have already been demonstrated with HVMAPS prototypes using two different approaches, firstly by using fast bipolar transistors for signal amplification [19] and secondly by using a pre-processed wafer with an internal gain layer [20]. Additionally, we are considering options based on low-gain avalanche detectors (LGAD) [21] or gaseous detectors with extreme time resolutions (PICOSEC) [22].

## 5 Sensitivity

The projected sensitivities of the future  $\mu^+ \rightarrow e^+ \gamma$  experiment with the expected performance of the detector technologies discussed in this document are estimated. Table 1 summarises the detector performance used in the sensitivity estimate. Five separate stopping targets are also assumed to further reduce the accidental backgrounds using the photon angle measured at the pair spectrometer. Figure 8 shows the projected sensitivity as a function of the beam rate. Three scenarios for the number of conversion layers are compared; one layer, four layers as the baseline and ten layers as an extreme case. Sensitivities down to  $(2 - 3) \times 10^{-15}$  are found to be reachable with a multi-layer photon converter at a beam rate above  $10^9 \mu^+/\text{s}$ .

## 6 Schedule

To optimize the use of time and resources, we are considering to adopt a staged approach, with a Phase-I experiment with limited performance but still improving the MEG II result, followed by a phase-II experiment to reach the final sensitivity.

In this scheme, the R&D for the photon and the positron timing detectors will continue in the next years. Their technical design could be completed soon after the end of the HIPA shutdown, foreseen in 2027-2028. In particular, a proof of principle of the conversion technique can be

Table 1: Summary of the detector resolutions and efficiencies used for the sensitivity estimate

Resolutions/efficiencies	
Photon energy	200 keV
Photon position	200 $\mu\text{m}$
Photon timing	30 ps
Photon angle	150 mrad
Photon detection efficiency (4 layers)	6 %
Positron energy	100 keV
Positron angle	6 mrad
Positron timing	30 ps
Positron detection efficiency	70 %
Geometrical acceptance	85 %

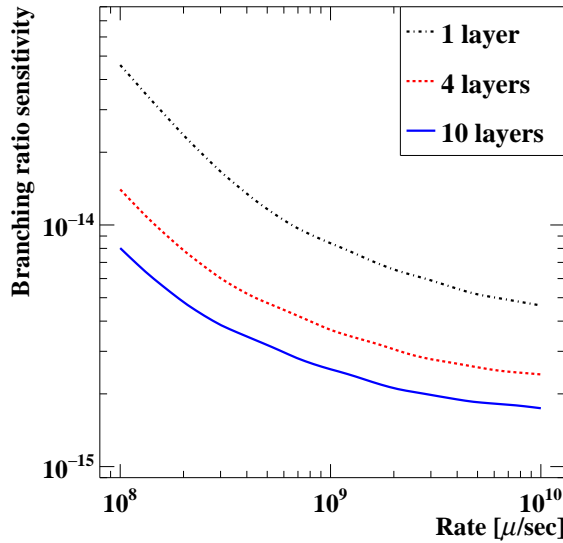
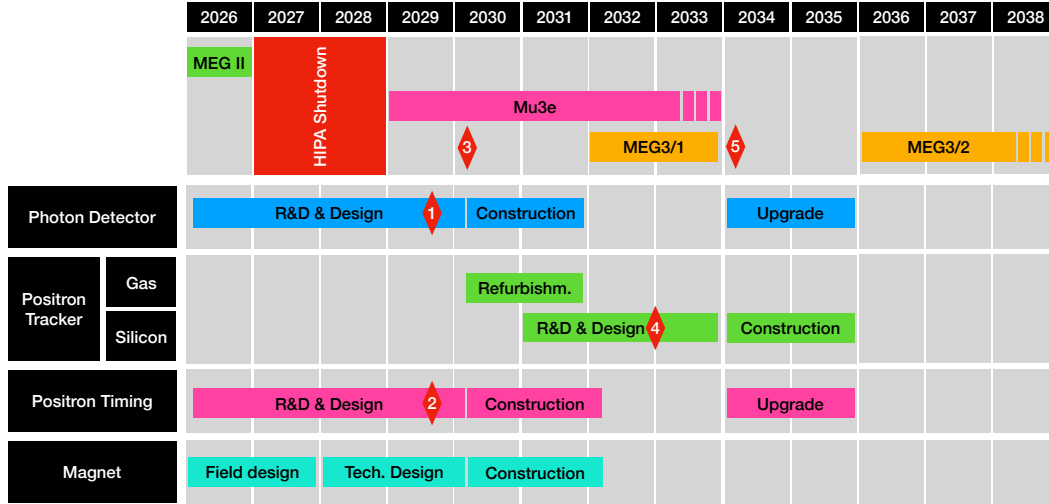


Figure 8: The projection of the branching ratio sensitivity (90% C.L. upper limit) for a 3-year run as a function of the beam rate for the experiment with the conversion pair spectrometer. Three scenarios for the number of conversion layers are compared.

obtained by performing a pion charge-exchange (CEX) experiment, where the reaction  $\pi^- + p \rightarrow \pi^0(\gamma\gamma) + n$  is produced and back-to-back  $\gamma\gamma$  pairs are selected to obtain almost monochromatic photons at 55 MeV. It will require a section of the conversion detector operated in a magnet, which could be COBRA or MEG II. This would lead to the construction of the phase-I experiment, running at  $\sim 10^8 \mu^+/\text{s}$  to make possible the use of a gaseous positron tracker (which could be a refurbished MEG II drift chamber) along with an almost complete version of the final photon and timing detectors. A sensitivity of a few  $10^{-14}$  could be reached. The actual value would be determined by the number of photon conversion layers and their acceptance, which in turn depends on the space availability within the magnet. To maximize the potential of the phase-I experiment, we could consider to design and build a dedicated magnet, to be reused in phase II. Alternatively, a descoped option based on the MEG II magnet could be also considered for phase I, and the new magnet would be produced later for phase II. Running at  $\sim 10^8 \mu^+/\text{s}$  in phase I would be feasible on the conventional HIPA  $\pi\text{E5}$  beam line, not in conflict with Mu3e running at HIMB.

In the meanwhile, Mu3e will pave the way toward a silicon positron tracker for  $\mu^+ \rightarrow e^+\gamma$ . The construction of this detector would follow the completion of the Mu3e experimental program, and minor upgrades of the other detectors could be performed in parallel. The phase-II  $\mu^+ \rightarrow e^+\gamma$  experiment, incorporating the new tracker, would be performed at HIMB in the second half of the next decade.



- ◆ 1: Photon converter proof of principle (CEX with converter + tracker in the MEG COBRA magnet)
- ◆ 2: Decision about positron timing technology
- ◆ 3: phase-I approval by PSI and funding agencies
- ◆ 4: Decision about positron tracker technology for phase-II
- ◆ 5: phase-II approval by PSI and funding agencies

Figure 9: A tentative schedule of the experimental program for a future  $\mu^+ \rightarrow e^+\gamma$  experiment in two phases (MEG3/1 and MEG3/2).

## THE STUDY GROUP FOR FUTURE $\mu^+ \rightarrow e^+\gamma$ EXPERIMENTS

Alessandro M. Baldini (INFN Pisa), Sei Ban (University of Tokyo), Laura Bees (Heidelberg Universität), Hicham Benmansour (INFN Pisa and Università di Pisa), Lorenzo Bianco (INFN Pisa and Università di Pisa), Gianluigi Boca (INFN Pavia and Università di Pavia), Paolo Walter Cattaneo (INFN Pavia), Gianluca Cavoto (INFN Roma and Sapienza Università di Roma), Fabrizio Cei (INFN Pisa and Università di Pisa), Marco Chiappini (INFN Pisa), Gianluigi Chiarello (Università di Palermo), Giovanni Dal Maso (CERN), Lorenzo Ferrari Barusso (INFN Genova and Università di Genova), Marco Francesconi (INFN Napoli), Matteo De Gerone (INFN Genova), Elisa Gabbrielli (INFN Roma and Sapienza Università di Roma), Luca Galli (INFN Pisa), Lukas Geritzen (University of Tokyo), Elia Giulio Grandoni (INFN Pisa and Università di Pisa), Marco Grassi (INFN Pisa), Malte Hildebrandt (PSI), Eloy Huidobro Rodriguez (Heidelberg Universität), Fedor Ignatov (University of Liverpool), Fumihito Ikeda (University of Tokyo), Toshiyuki Iwamoto (University of Tokyo), Tamasi Kar (Heidelberg Universität), Francesco Leonetti (INFN Pisa and Università di Pisa), Ljiljana Morvaj (PSI), Satoshi Mihara (KEK), Toshinori Mori (University of Tokyo), Hajime Nishiguchi (KEK), Wataru Ootani (University of Tokyo), Atsushi Oya (University of Tokyo), Angela Papa (INFN Pisa and Università di Pisa), Daniele Pasciuto (INFN Roma), Marco Panareo (INFN Lecce and Università di Lecce), Francesco Renga (INFN Roma), Rei Sakakibara (University of Tokyo), Susanna Scarpellini (INFN Roma and Sapienza Università di Roma), André Schöning (Heidelberg Universität), Yusuke Uchiyama (KEK), Antoine Venturini (INFN Pisa and University of Pisa), Cecilia Voena (INFN Roma and Sapienza Università di Roma), Rintaro Yokota (University of Tokyo).

## References

- [1] L. Calibbi, G. Signorelli, Charged lepton flavour violation: An experimental and theoretical introduction. *Riv. Nuovo Cim.* **41**(2), 71–174 (2018). doi:[10.1393/ncr/i2018-10144-0](https://doi.org/10.1393/ncr/i2018-10144-0)
- [2] S. Mihara et al., Charged Lepton Flavor-Violation Experiments. *Ann. Rev. Nucl. Part. Sci.* **63**, 531–552 (2013). doi:[10.1146/annurev-nucl-102912-144530](https://doi.org/10.1146/annurev-nucl-102912-144530)
- [3] K. Afanaciev et al. (MEG II), A search for  $\mu^+ \rightarrow e^+\gamma$  with the first dataset of the MEG II experiment. *Eur. Phys. J. C* **84**(3), 216 (2024). doi:[10.1140/epjc/s10052-024-12416-2](https://doi.org/10.1140/epjc/s10052-024-12416-2), arXiv:[2310.12614](https://arxiv.org/abs/2310.12614). [Erratum: *Eur.Phys.J.C* 84, 1042 (2024)]
- [4] K. Arndt et al., Technical design of the phase I Mu3e experiment (2021), arXiv:[2009.11690](https://arxiv.org/abs/2009.11690)
- [5] B. L. et al., Mu2e Technical Design Report (2015), arXiv:[1501.05241](https://arxiv.org/abs/1501.05241)
- [6] R. Abramishvili et al. (COMET), COMET Phase-I Technical Design Report. *PTEP* **2020**(3), 033C01 (2020). doi:[10.1093/ptep/ptz125](https://doi.org/10.1093/ptep/ptz125), arXiv:[1812.09018](https://arxiv.org/abs/1812.09018)
- [7] A. M. Baldini et al. (MEG II Collaboration), The design of the MEG II experiment. *Eur. Phys. J. C* **78**(5) (2018). doi:[10.1140/epjc/s10052-018-5845-6](https://doi.org/10.1140/epjc/s10052-018-5845-6)
- [8] K. Afanaciev et al. (MEG II), Operation and performance of the MEG II detector. *Eur. Phys. J. C* **84**(2), 190 (2024). doi:[10.1140/epjc/s10052-024-12415-3](https://doi.org/10.1140/epjc/s10052-024-12415-3), arXiv:[2310.11902](https://arxiv.org/abs/2310.11902)
- [9] R. Eichler, et al., IMPACT conceptual design report. PSI Bericht, Report No.: 22-01 (2022). <https://www.dora.lib4ri.ch/psi/islandora/object/psi%3A41209>
- [10] Z. Hodge, Production, Characterization, and Monitoring of Surface Muon Beams for Charged Lepton Flavor Violation Experiments. Doctoral thesis, ETH Zurich, Zurich, 2018
- [11] F. A. Berg, CMBL - A High-Intensity Muon Beam Line & Scintillation Target with Monitoring System for Next-Generation Charged Lepton Flavour Violation Experiments. Doctoral thesis, ETH Zurich, Zurich, 2017
- [12] M. Aiba et al., Science Case for the new High-Intensity Muon Beams HIMB at PSI (2021), arXiv:[2111.05788](https://arxiv.org/abs/2111.05788)
- [13] G. Dal Maso, Optimization of the High-Intensity Muon Beamlines for MEG II, Mu3e and HIMB. Doctoral thesis, ETH Zurich, Zurich, 2024
- [14] A. Baldini et al. (MEG II Collaboration), MEG upgrade proposal (2013), arXiv:[1301.7225](https://arxiv.org/abs/1301.7225)
- [15] I. Peric, A novel monolithic pixelated particle detector implemented in high-voltage CMOS technology. *Nucl. Instrum. Meth. A* **582**, 876–885 (2007). doi:[10.1016/j.nima.2007.07.115](https://doi.org/10.1016/j.nima.2007.07.115)
- [16] A. Papa et al., Towards large calorimeters based on Lanthanum Bromide or LYSO crystals coupled to silicon photomultipliers: A first direct comparison for future precision physics. *Nucl. Instrum. Meth. A* **1049**, 167997 (2023). doi:[10.1016/j.nima.2022.167997](https://doi.org/10.1016/j.nima.2022.167997)

- [17] G. Cavoto et al., The quest for  $\mu \rightarrow e\gamma$  and its experimental limiting factors at future high intensity muon beams. *Eur. Phys. J. C* **78**(1) (2018). [doi:10.1140/epjc/s10052-017-5444-y](https://doi.org/10.1140/epjc/s10052-017-5444-y), [arXiv:1811.12324](https://arxiv.org/abs/1811.12324)
- [18] A. Schöning et al., MuPix and ATLASPix – Architectures and Results. *PoS Vertex2019*, 024 (2020). [doi:10.22323/1.373.0024](https://doi.org/10.22323/1.373.0024), [arXiv:2002.07253](https://arxiv.org/abs/2002.07253)
- [19] F. Martinelli et al., Measurements and analysis of different front-end configurations for monolithic SiGe BiCMOS pixel detectors for HEP applications. *JINST* **16**(12), P12038 (2021). [doi:10.1088/1748-0221/16/12/P12038](https://doi.org/10.1088/1748-0221/16/12/P12038), [arXiv:2111.11184](https://arxiv.org/abs/2111.11184)
- [20] M. Milanesio et al., Gain measurements of the first proof-of-concept PicoAD prototype with a  $^{55}\text{Fe}$  X-ray radioactive source. *Nucl. Instrum. Meth. A* **1046**, 167807 (2023). [doi:10.1016/j.nima.2022.167807](https://doi.org/10.1016/j.nima.2022.167807)
- [21] T. Croci et al., Development and test of innovative Low-Gain Avalanche Diodes for particle tracking in 4 dimensions. *Nucl. Instrum. Meth. A* **1047**, 167815 (2023). [doi:10.1016/j.nima.2022.167815](https://doi.org/10.1016/j.nima.2022.167815)
- [22] J. Bortfeldt et al., PICOSEC: Charged particle timing at sub-25 picosecond precision with a Micromegas based detector. *Nucl. Instrum. Meth. A* **903**, 317–325 (2018). [doi:10.1016/j.nima.2018.04.033](https://doi.org/10.1016/j.nima.2018.04.033), [arXiv:1712.05256](https://arxiv.org/abs/1712.05256)